Dynamic Surface Modification of Metal–Organic Framework Nanoparticles via Alkoxyamine Functional Groups

Simon Spiegel, Ilona Wagner, Salma Begum, Matthias Schwotzer, Isabelle Wessely, Stefan Bräse, and Manuel Tsotsalas*

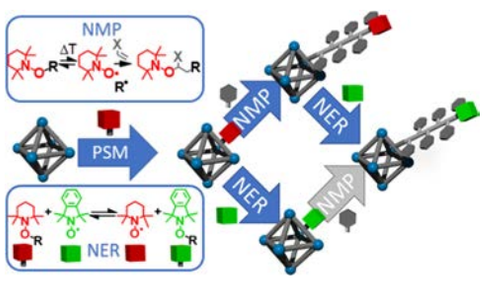

ABSTRACT: External surface engineering of metal–organic framework nano particles (MOF NPs) is emerging as an important design strategy, leading to optimized chemical and colloidal stability. To date, most of the MOF surface modifications have been performed either by physical adsorption or chemical association of small molecules or (preformed) polymers. However, most of the currently employed approaches cannot precisely control the polymer density, and dynamic modifications at the surfaces on demand have been a challenging task. Here, we introduce a general approach based on covalent modification employing alkoxyamines as a versatile tool to modify the outer surface of MOF nanoparticles (NPs). The alkoxyamines serve as initiators to grow polymers from the MOF surface via nitroxide mediated polymerization (NMP) and allow dynamic attachment of small molecules via a nitroxide exchange reaction (NER). The successful surface modification and successive surface polymerization are confirmed via time of flight secondary ion mass spectrometry (ToF SIMS), size exclusion chromatography (SEC), and nuclear magnetic resonance (NMR) spectroscopy. The functionalized MOF NPs exhibit high suspension stability and good dispersibility while retaining their chemical integrity and crystalline structure. In addition, electron paramagnetic resonance spectroscopy (EPR) studies prove the dynamic exchange of two different nitroxide species via NER and further allow us to quantify the surface modification with high sensitivity. Our results demonstrate that alkoxyamines serve as a versatile tool to dynamically modify the surface of MOF NPs with high precision, allowing us to tailor their properties for a wide range of potential applications, such as drug delivery or mixed matrix membranes.

INTRODUCTION

Metal–organic framework nanoparticles (MOF NPs) are an emerging class of modular materials due to their outstanding versatility in chemical composition and functionality, com bined with their tunable porosity and well defined crystalline structures.[1,2] MOFs show promise for diverse applications, ranging from catalysis,[3,4] organic electronics,[5,6] gas storage and separation[7,8] to biology and medicine.[9−12] A crucial factor in the interaction with the surrounding media is the chemistry on the external surface of MOF particles. Precise control over external surface functionalization enables us to achieve selective interfacial interactions, improved compatibility, and well dispersed stable colloidal suspensions of MOF NPs. Therefore, the chemistry of the external surface is a powerful tool and an important factor for the performance of MOF NPs in many of the aforementioned applications.[13] A common drawback in the processing and application of MOF NPs is their tendency to aggregate. To avoid aggregation of MOF nanoparticle suspensions, the surface chemistry must be precisely adjusted to the polarity of the desired solvents. Adjusting the surface chemistry is a common strategy, for example, in the creation of stable suspensions[10,14] or mixed matrix membranes.[15] In the case of stable suspensions, the interaction with the solvent molecules is enhanced, which reduces aggregation and sedimentation. Analogue principles are valid for the interaction of MOF with polymers.[16,17] A stable dispersion allows a homogeneous inclusion of the NPs in the polymer matrix. In addition, adjusting the surface chemistry of the MOFs to the polymer matrix avoids phase separation at the particle/polymer interface.[18,19] Other examples where surface chemistry of NPs plays an important role are biological and medical applications, e.g., controlling the adsorption of biomolecules for imaging or drug delivery.

To introduce various functionalities to the external surfaces of MOF NPs via postsynthetic modifications, coordination functionalization at metal nodes and covalent bond formation at prefunctionalized organic linkers as well as their remaining anchoring group (i.e., COOH) can be utilized.[10,20] Further strategies for postsynthetic modifications are metal and linker

exchange.[21] Therefore, linker molecules are often designed to contain functional groups as a starting point for further modifications. Due to the porous character of MOF NPs, postsynthetic modifications can be designed to target both the inner surface (pores/framework) and the outer surface (particle surface). The employed surface modification strategy ideally preserves the attractive features of MOFs, i.e., high variability combined with a precise crystalline structure, and combines it with a well defined and dynamic or reversible surface chemistry.[22]

Here, we introduce external surface modifications of MOF NPs based on employing alkoxyamine functional groups. Alkoxyamines are molecules containing a C−ON bond. Under thermal conditions, this bond can be cleaved homolytically, leading to a persistent nitroxide radical and a transient carbon radical. These two radical species can reform the alkoxyamine in a dynamic process.[23,24] Nitroxide mediated polymerization (NMP) employs alkoxyamines as initiators as well as mediators for polymerization.[24,25] NMP is a well known method belonging to the group of reversible deactivation radical polymerization (RDRP).[26] NMP enables the precise synthesis of complex highly functional macromolecular structures[27] and can be used as a method for controlled surface modification.[28] While initially limited to styrene, modification of the nitroxide radical allows us to apply NMP for a wide range of monomer types.[27,29] In addition to NMP, reversible homolysis of alkoxyamines can also be employed in the nitroxide exchange reaction (NER), belonging to the class of dynamic covalent chemistry.[30,31] In NER, the C−ON bond homolysis of the alkoxyamine is performed in the presence of an additional nitroxide radical species. The dynamic exchange between the two nitroxide species leads to a thermodynamically controlled product of the reaction. NER was employed in surface modification, as well as in the creation of dynamic macro molecular architectures and porous frameworks, through a combination of multivalent alkoxyamines with multivalent nitroxide radicals in the exchange reaction.[32−36] Surface modification of MOF NPs with alkoxyamines allows us to employ both NMP and NER to modify their surface chemistry precisely and dynamically.

In this investigation, we have chosen UiO 66 NH_2 as a model system to study the surface functionalization of MOF NPs as this MOF type is well established, readily accessible, and possesses high chemical stability. UiO 66 NH_2 belongs to the group of the Zr based UiO type MOFs,[37,38] well known for their exceptional thermal and chemical stability. Importantly, the amino groups are employed for initial alkoxyamine modifications, as shown in Figure 1.[39,40] Figure 1 shows a schematic overview of the alkoxyamine functionalization of MOF NPs and successive surface modification via the NER, as well as controlled surface polymerization via NMP.

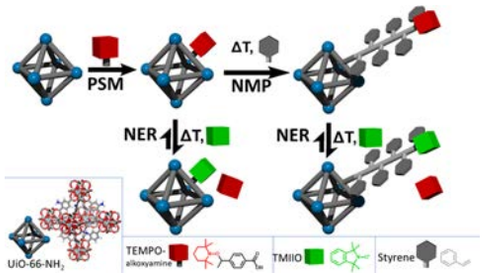

Figure 1. Schematic overview of the alkoxyamine surface modification strategy for MOF NPs. After attachment of TEMPO alkoxyamine to the surface, the TEMPO nitroxide (red) can be dynamically exchanged with the TMIIO nitroxide (green) in a nitroxide exchange reaction (NER). In addition, alkoxyamines can serve as initiators for nitroxide mediated polymerization (NMP). After polymerization, the alkoxyamine function remains active, as demonstrated by successive NER after NMP.

EXPERIMENTAL SECTION

Characterization. Pristine, alkoxyamine modified, and PS func tionalized UiO 66 NH_2 NPs were characterized by powder X ray diffraction (PXRD, Bruker D8 Advance), thermogravimetric analysis (TGA), scanning electron microscopy (SEM, Quattro S ESEM by Thermo Scientific), attenuated total reflection−infrared (ATR−IR) spectroscopy, time of flight secondary ion mass spectrometry (ToF SIMS), dynamic light scattering (DLS), and electron paramagnetic resonance (EPR). The porosity of the nanoparticles was analyzed by argon sorption measurements and BET analysis. Nuclear magnetic resonance (NMR) and size exclusion chromatography (SEC) were performed to determine the molecular weight distribution and the polydispersity index (PDI) of the PS polymer. Technical details of all of the characterization methods are provided in the Supporting Information.

Materials. Acetic acid, aluminum oxide (basic), dimethylforma mide (DMF), 1 ethyl 3 (3 dimethylaminopropyl)carbodiimide hy drochloride (EDC·HCl), *N,N,N′,N″,N″* pentamethydietylentriamine (PMDTA), styrene, and *N* hydroxysulfosuccinimide (sulfo NHS) were purchased from Sigma Aldrich (Germany); 2 aminoterephthalic acid (BDC NH_2), 4 (1 bromoethyl)benzoic acid, CuBr, Cu powder, EDTA·$2H_2O$, (2,2,6,6 tetramethylpiperidine 1 yl)oxyl (TEMPO) (free radical), tetrahydrofuran (THF) (unstabilized), and $ZrCl_4$ were obtained from Alfa Aesar; and dichloromethane (DCM), ethanol (absolute), $MgSO_4$, and toluene were purchased from VWR.

Styrene was purified by passing it through a basic aluminum oxide column to remove the stabilizers. The cleaned styrene was degassed three times via freeze−pump−thaw cycles prior to use and stored under nitrogen at −22 °C to prevent self polymerization. The same procedure was used to degas other liquids if needed. All other chemicals were used as received.

Synthesis of TEMPO Alkoxyamine. TEMPO alkoxyamine was synthesized according to a literature procedure[41] with little modification in the purification step. A two neck round bottom flask, equipped with a reflux condenser was charged with 4 (1 bromoethyl)benzoic acid (1.20 equiv, 7.68 mmol, 1.76 g), TEMPO (1.00 equiv, 6.40 mmol, 1.00 g), CuBr (1.20 equiv, 7.68 mmol, 1.10 g), and copper powder (1.20 equiv, 7.68 mmol 0.49 g). Under inert conditions, the degassed liquid components, PMDTA (2.41 equiv, 15.4 mmol, 3.21 mL) and THF (30.0 mL), were added. The resulting reaction mixture was refluxed at 80 °C for 24 h. After cooling, the mixture was diluted with 100 mL of DCM and extracted with a saturated aqueous Na_2EDTA solution until the copper catalyst was completely removed from the organic phase, resulting in a colorless aqueous phase. The organic phase was dried over $MgSO_4$ before removing the solvent under reduced pressure to produce a yellow crude product with a purity of 95% (analyzed by ^1H NMR). For further purification, the crude product was washed with cold methanol (−22 °C). The clean product was obtained as a white solid (yield: 1.58 g, purity 98%, by ^1H NMR).

Synthesis of UiO-66-NH_2 NPs. UiO 66 NH_2 NPs were synthesized by a solvothermal procedure reported by Schaate et al. in 2011.[42] In a vial, $ZrCl_4$ (1.00 equiv, 1.03 mmol, 240 mg), acetic acid (30.0 equiv, 30.9 mmol, 1.77 mL), and water (4.00 equiv, 4.12 mmol, 75.0 μL) were added to 20 mL of DMF. In a second vial, BDC NH_2 (1.00 equiv, 1.03 mmol, 186 mg) was dissolved in 40 mL of DMF. Both solutions were sonicated (∼15 min) till a clear solution was achieved. Thereafter, both solutions were combined in a crimp vial capped with an aluminum cap equipped with a Teflon septum and heated in an oven at 120 °C for 24 h. After cooling to room temperature, the NPs were collected via centrifugation and washed

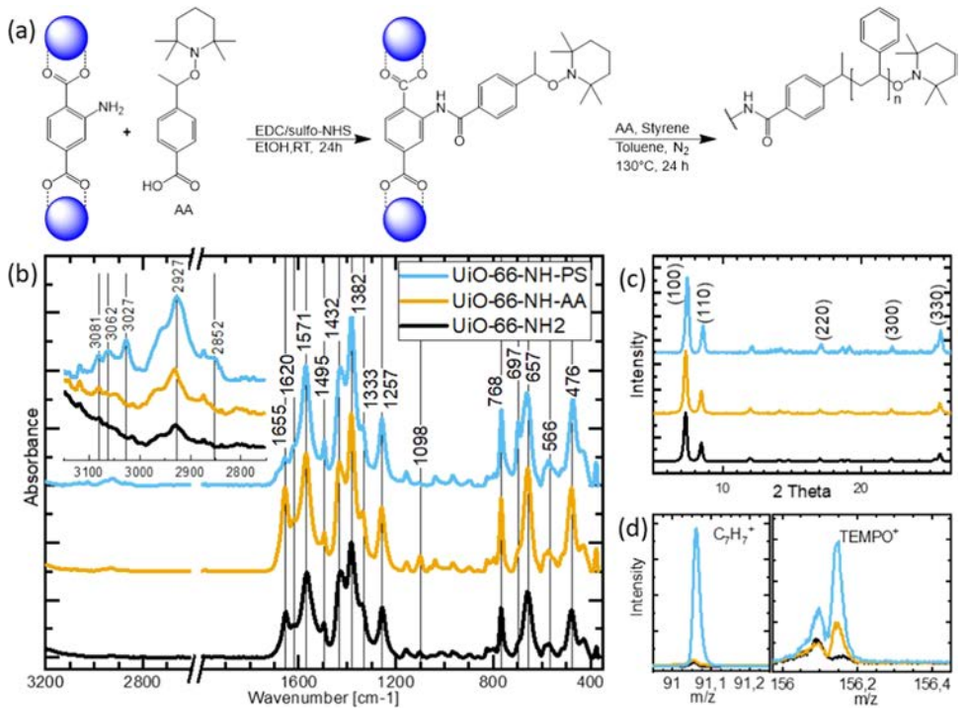

Figure 2. Overview of MOF nanoparticle modifications. (a) Reaction scheme of UiO 66 NH_2 successive surface modification with alkoxyamines and polystyrene; the blue spheres represent the $[Zr_6O_4(OH)_4]^{12+}$ clusters. Characterization of the pristine MOF UiO 66 NH_2 (black), alkoxyamine modified MOF UiO 66 NH AA (orange), and polystyrene functionalized MOF UiO 66 NH PS (blue) by (b) ATR−IR, (c) PXRD, and (d) ToF SIMS showing $C_7H_7^+$ and $TEMPO^+$ signals (due to overlapping, a minute offset was applied to the orange signals to increase the visibility of the black signals).

three times with DMF and three times with EtOH (20 mL). The resulting pale yellow product (175 mg) was suspended in ethanol and stored as an ethanol suspension until further use.

Surface Modification of UiO-66-NH_2 NPs with Alkoxyamine (UiO-66-NH-AA). In a round bottom flask, TEMPO alkoxyamine (1.00 equiv, 0.04 mmol, 12.2 mg) was dissolved in ethanol (10 mL). Afterwards, sulfo NHS (1.20 equiv, 0.05 mmol, 10.4 mg) and EDC·HCl (6.00 equiv, 0.24 mmol, 46.0 mg) were added to the solution and stirred until all components were completely dissolved. The UiO 66 NH_2 suspension (100 mg in 10 mL of EtOH) was added to the reaction mixture and stirred at room temperature for 24 h. The alkoxyamine modified MOF particles were collected via centrifugation and washed three times with EtOH. The obtained alkoxyamine (AA) modified MOF particles were suspended and stored in EtOH.

Surface Functionalization of UiO-66-NH-AA NPs with Polystyrene (UiO-66-NH-PS). A 25 mL Schlenk tube with a magnetic stir bar was charged with UiO 66 NH AA (100 mg), TEMPO alkoxyamine (1.00 equiv, 0.33 mmol 100 mg), styrene (100 equiv, 32.8 mmol, 3.79 mL), and toluene (4.40 mL). The reaction mixture was then carefully degassed three times via the freeze−pump−thaw method, backfilled with nitrogen, sealed, and heated at 130 °C for 24 h under vigorous stirring. Thereafter, the reaction mixture was removed from the oil bath and cooled to room temperature. Immediately after completion of the reaction, 0.10 mL of the sample was withdrawn from the warm reaction mixture to analyze the conversion of styrene by NMR. The cooled reaction mixture was stirred and diluted dropwise with ethanol until the observation of polystyrene precipitation. The reaction mixture was centrifuged, and the collected precipitates were washed with a mixture of toluene and ethanol (5:3 V/V, 4 × 20 mL). The supernatant was checked for polystyrene via dropping in an excess amount of ethanol and collected for further characterization. The washed particles were stored in a suspension, in ethanol, and in toluene for characterization.

In a one pot approach, an analogue synthesis was performed using the unmodified UiO 66 NH_2 NPs.

RESULTS AND DISCUSSION

Surface modification of UiO 66 NH_2 with alkoxyamine was performed via amide bond formation using EDC/sulfo NHS, and successive polymerization was performed via NMP. The overall reaction scheme is shown in Figure 2a. The styrene polymerization is initiated from the alkoxyamine units fixed on UiO 66 NH_2. In parallel to this, a bulk polystyrene (PS) polymer was formed in situ with the addition of alkoxyamine in the reaction mixture. In the following, we will refer to the bulk polystyrene formed in solution as reference PS. To confirm the successful attachment of alkoxyamine and successive surface polymerization while maintaining the parent MOF NPs' structural integrity during the functionalization process, we used different characterization methods (see Figure 2).

We performed ATR−IR spectroscopy for each sample, as shown in Figure 2b, to identify their chemical composition. The spectra of UiO 66 NH_2 and UiO 66 NH AA differ mainly in their relative intensity of different bands and are discussed together. The bands at 1656 and 1098 cm^{-1} belong to the C═O stretch and C−H bend vibrations of the remaining DMF inside the pores, respectively. The bands at 1620 and 1571 cm^{-1} stem from the C−N stretch and the symmetric in plane bending of the N−H bonds. The bands at 1495, 1382, and 1257 cm^{-1} belong to the in plane bending of C−H and the corresponding C═C−C ring vibration. The C−H out of plane bending from the linker is visible at 768 cm^{-1}. The bands at 659, 569, and 476 cm^{-1} belong to the Zr cluster vibrations: μ_3−O, Zr−(CO) (asymmetric), and μ_3−OH stretch, respectively. The band at 1432 cm^{-1} can be assigned to the O−H stretch of the clusters. The only significant new band, which is pronounced in the spectrum of UiO 66 NH PS (blue), appears at 697 cm^{-1}, corresponding to the C−H out of plane

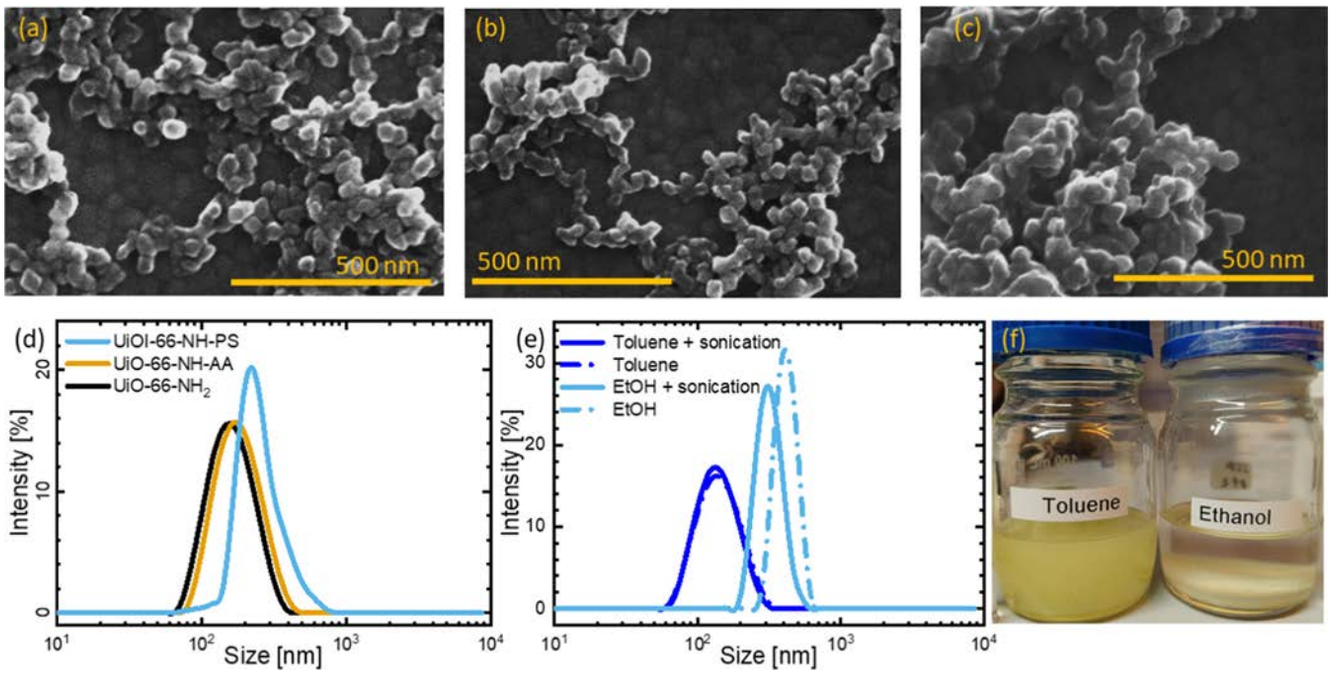

Figure 3. Characterization of MOF nanoparticle size. (a–c) SEM images of the MOF NPs: UiO 66 NH_2, UiO 66 NH AA, and UiO 66 NH PS, respectively. (d, e) DLS measurement of UiO 66 NH PS in ethanol and in toluene: UiO 66 NH_2, (black), UiO 66 NH AA (orange), and UiO 66 NH PS (in ethanol/toluene) (light/dark blue); the dotted line represents as prepared particles, and the solid line represents particles after 30 min of sonication. (f) Optical image of UiO 66 NH PS NPs suspended in toluene and ethanol. (Note: samples are drop cast on the gold coated Si wafer for SEM imaging. The darker, less resolved structures in the background of the SEM images represent the gold substrate).

vibrations of aromatic hydrogens. Upon closer examination at the region of 2700–3100 cm^{-1}, several new signals at 2852, 2927, 3027, 3062, and 3081 cm^{-1} can be seen. The signals at wavenumbers greater than 3000 cm^{-1} are characteristic of monosubstituted aromatic rings and correspond to C–H stretch vibrations. They therefore strongly point toward the successful polymerization of polystyrene.

The particles functionalized in the one pot synthesis show an ATR–IR spectrum equivalent to the one shown for UiO 66 NH PS. This points toward an in situ functionalization of the particles, either via amide formation at the linkers[39] or coordination to the metal site at elevated temperature.[10,40]

We confirmed the presence of TEMPO end groups in UiO 66 NH AA as well as in UiO 66 NH PS via ToF SIMS measurements (Figure 2d). Both spectra show a signal at 156.24 m/z, corresponding to $TEMPO^+$ ions. The spectrum of UiO 66 NH PS shows a characteristic signal at 91.06 m/z corresponding to tropylium ions ($C_7H_7^+$), confirming the presence of polystyrene on the surface. The spectrum of UiO 66 NH_2 shows only baseline signals in both cases.

To ensure that the crystallinity of the MOF particles is retained throughout the modifications, we recorded PXRD patterns for each step (Figure 2c). All samples showed the characteristic PXRD pattern of UiO 66 NH_2, which matched well with the reference pattern. The relatively strong signals at 2θ = 7.32, 8.44, 17.0, 22.2, and 25.7° were labeled with the corresponding (100), (110), (220), (300), and (330) planes. The lattice distances calculated from these angles are very consistent at 1.04 and 1.21 nm for the 110 and 100 directions, respectively. All observed 2θ signals are consistent with those of the pristine UiO 66 NH_2; therefore, it can be concluded that topological and crystalline characteristics are retained throughout the modifications.[38,43]

To verify the retention of the three dimensional (3D) porous structure of UiO 66 NH_2 after the polymerization, argon (Ar) sorption isotherms were collected at 87 K for UiO 66 NH_2 and UiO 66 NH PS. As shown in supporting information Figure S16, both samples exhibit a type I sorption isotherm, which is characteristic of microporous materials. For UiO 66 NH_2, the Brunauer–Emmett–Teller (BET) surface area of 1236 m^2/g with a pore size of 1–2 nm and a pore volume of 0.622 cm^3/g is found to be in good agreement with the values reported for UiO 66 NH_2 with high defect density.[44] For UiO 66 NH PS, a BET surface area of 694 m^2/g with an average pore size of 1 nm and a pore volume of 0.275 cm^3/g is found. A decrease of close to 49% in the surface area observed in UiO 66 NH PS is partly attributed to the comparative mass increase caused by the polymer coverage on the MOF particles. The lack of the 2 nm pores and the decrease in the surface area after NMP may be due to healing of crystal defects at high temperatures or the result of polymerization inside the larger (2 nm) pores.

For investigation of particle size and suspension stability before and after modification, we performed SEM and DLS measurements (see Figure 3).

As shown in the SEM images in Figure 3a–c, the NPs exhibit a narrow size distribution. The particle size of the pristine UiO 66 NH_2 NPs ranges from 60 to 100 nm in diameter. After the attachment of alkoxyamine and surface polymerization with PS via NMP (UiO 66 NH AA and UiO 66 NH PS, respectively), the parent octahedron morphology and particle size distribution are retained. The slightly rounded edges observed in the case of UiO 66 NH PS suggest that the polymer formation is successfully carried out on the surface of MOF NPs.

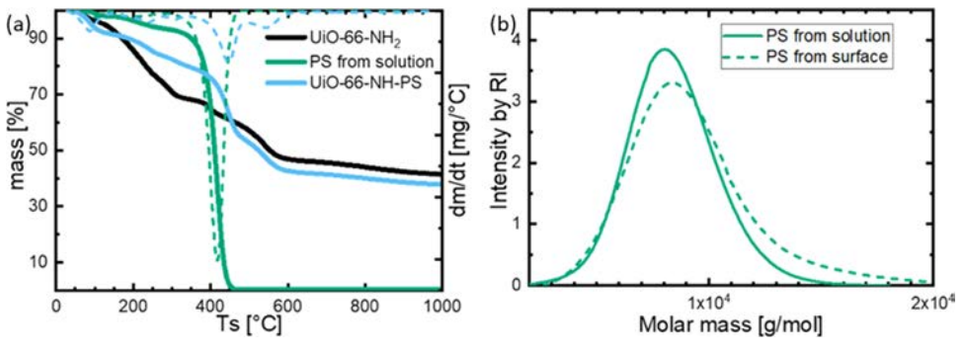

Figure 4. Characterization of the surface polymer. (a) TGA of pristine UiO 66 NH_2 (black), polystyrene formed in situ as the bulk polymer in the reaction mixture (green), and UiO 66 NH PS (blue). (b) SEC analysis of polystyrene from the surface of UiO 66 NH PS compared to the reference polystyrene formed in situ in the reaction mixture.

The DLS measurement of the UiO 66 NH_2 particles shown in Figure 3d–e reveals a narrow size distribution with an average particle size of 130 nm, which is in good agreement with the SEM results. The surface modification resulted in a slight increase of about 20 nm in average size for the UiO 66 NH AA particles. This indicates a higher aggregation tendency of the alkoxyamine modified particles compared to the unmodified pristine MOF NPs. The measurement of UiO 66 NH PS in ethanol shows strong agglomeration or sedimentation during the measurement, indicating a successful surface modification with apolar polystyrene, whereas the DLS measurements of the PS functionalized particles (UiO 66 NH PS) in toluene show a narrow size distribution with an average particle size of around 130 nm, indicating well dispersed NPs. The UiO 66 NH PS particles tend to have a stable suspension in toluene, as confirmed by repeated measurements after 30 min of sonication. The PS surface modification via NMP therefore successfully modulated the surface characteristics of MOF NPs, leading to a high stability in apolar solvents and a poor stability in polar solvents. This is also shown in the optical image in Figure 3f, which was taken after letting the suspension rest for a week.

To quantify the amount of the surface polymer and to determine its molecular weight and dispersity, TGA and SEC measurements were performed (Figure 4).

TGA measurements are shown in Figure 4a. The main mass loss of polystyrene takes place in the region from 300 to 500 °C. Alkoxyamine decomposes at lower temperatures of around 150–200 °C. The mass loss due to alkoxyamine could not be observed for UiO 66 NH AA, as the single layer of alkoxy amine on the surface does not contribute enough to the overall mass of the particles to be observable. Also, the mass loss due to small molecules in the pores (e.g., solvents) may outweigh the minuscule mass loss due to the surface modification. TGA graphs of UiO 66 NH PS, compared to pristine UiO 66 NH_2 and the PS reference polymer synthesized in situ in the reaction mixture, revealed a mass loss of around 16% contributed by PS. Losses were calculated by comparing the mass loss at 300 °C to the mass loss at 500 °C for each measurement. The difference between these steps was used to calculate the mass loss due to the decomposition of PS.

NMR measurements of the sample taken from the reaction mixture revealed a conversion of about 73%. To obtain the molecular weight of the in situ synthesized reference polymer in the reaction mixture, as well as the polymer on the MOF surface, both were analyzed by SEC. The surface polymer of UiO 66 NH PS was collected by decomposing the MOF with aqueous sodium hydroxide. From this solution, the polymer was extracted by THF. SEC measurements of the extracted surface polymer are shown in Figure 4b and revealed a molecular weight M_W of 8392 g/mol. This is in good agreement with the measured molecular weight of 7890 g/mol of the reference polymer formed in situ in the reaction mixture (Table 1). The small difference in molecular weight is partially attributed to the attachment of alkoxyamine to the MOF linker, which increases the M_W of the chain by approximately 180 g/mol. The molecular weights correspond to a chain length of 76 and 73 repeating units for the surface and reference polymers, respectively, which is in good agreement with the conversion determined by NMR.

Table 1. PS Polymer Properties Analyzed by SEC

	M_W [g/mol]	M_N [g/mol]	Đ
reference PS	7890	7316	1079
surface PS	8392	7638	1099

Besides the surface modification via NMP, the nitroxide exchange reaction (NER) is further employed to introduce a new functionality to the surface. NERs were performed by exchanging the TEMPO nitroxide of the alkoxyamine with TMIIO nitroxide (2 lambda1 oxidanyl 1,1,3,3 tetramethyli soindole) added in the solution. For comparison, we performed the NER with the alkoxyamine in solution, the alkoxyamine surface modified MOF particles, and PS function alized MOF particles. The exchange was studied via EPR spectroscopy; both TEMPO and TMIIO nitroxide species show a different hyperfine coupling constant.[31] The successful release of TEMPO radicals was observed in all three cases, thereby proving exchange with TMIIO. A scheme of the exchange process, the spectra of the pure compounds (TEMPO and TMIIO), and the spectra of the exchange reactions are shown in Figure 5.

The free radicals TEMPO and TMIIO are EPR active, whereas the bound components, the alkoxyamines, are EPR silent. During the NER, free TMIIO is exchanged with the bound TEMPO, which is thereby released into the solution and can then be detected by EPR. The two single component spectra (Figure 5b) are fitted to the mixed spectra (Figure 5c–e). The weight of the two fitted components is directly related to the relative concentration of the two measured components. As shown by the analysis of the EPR spectrum for the exchange reaction in solution (Figure 5c), the equilibrium condition for a 1:1 (n:n) ratio does not lead to a 1:1 (n:n) ratio of free

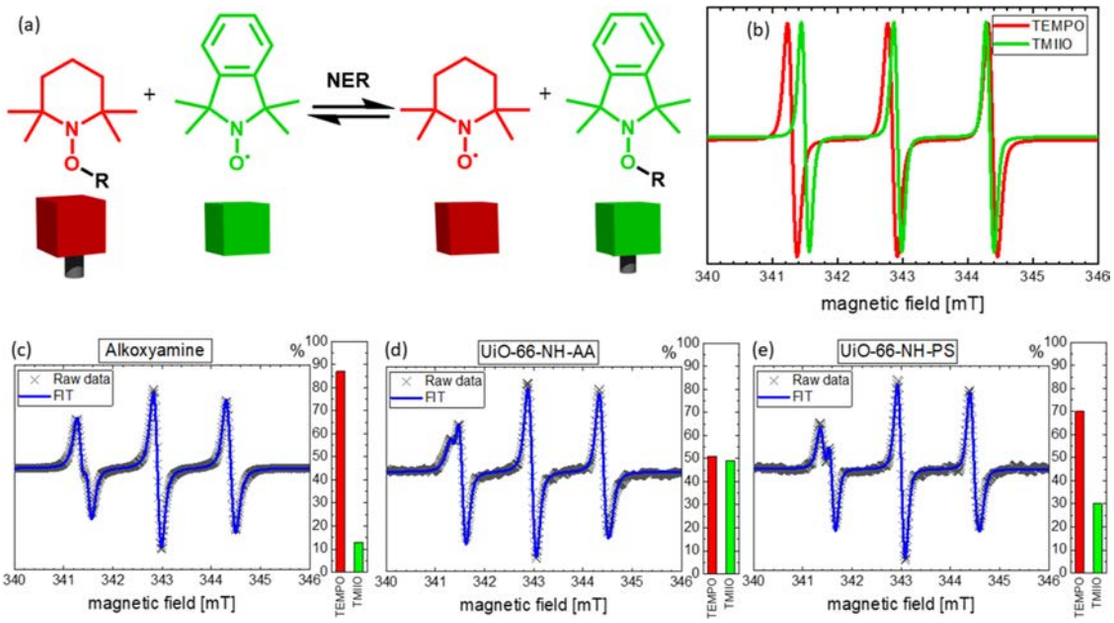

Figure 5. Nitroxide exchange reaction of UiO 66 NH AA and UiO 66 NH PS: (a) scheme of the exchange process, (b) reference spectra of TEMPO (red) and TMIIO (green) nitroxides in solution, and (c−e) EPR spectra after the exchange of the TEMPO nitroxide with TMIIO nitroxide for free alkoxyamine in solution, UiO 66 NH AA, and UiO 66 NH PS, respectively. Red and green bars represent the percentage of free TEMPO and TMIIO in solution.

TEMPO to TIMIIO in solution. This is due to the different stabilities of the corresponding alkoxyamines and is consistent with previous results.[31] From the relative weight of the single components fitted to the measurements (Figure 5d−e), the amount of TEMPO on the surface is approximated (for further details on the surface coverage evaluation, see Table 2 and SI).

Table 2. Overview of Calculations Based on EPR and Their Comparison to TGA Results

	coverage by EPR [pmol/cm^2]	coverage by EPR [%]	mass by EPR [%]	mass by TGA [%]
UiO-66-NH-AA	17.8	8	0.20	<3%
UiO-66-NH-PS	12.3	5	3.42	16.0

The calculations show a coverage of TEMPO on the surface of 17.8 pmol/cm^2 (8%) and 12.3 pmol/cm^2 (5%) for UiO 66 NH AA and UiO 66 NH PS, respectively. The calculated masses of the modifications are by a factor of 5 lower than the masses inferred from TGA measurements. Therefore, we conclude that though qualitatively confirming the availability of the functional groups, the actual surface coverage may be higher than that implied by the calculations based on EPR.

CONCLUSIONS

We have developed a general protocol to dynamically modify the surface properties of MOF NPs by employing alkoxyamine functional groups. Our approach allows controlled polymerization via NMP and incorporation of functional molecules on demand via NER.

Our studies confirm the successful surface modification of UiO 66 NH_2 with alkoxyamines and surface functionalization with polystyrene of controlled chain length and low dispersity. SEC measurements showed a good correlation of the polymers formed in solution and on the particle surface. The low dispersity of around 1.1 confirms that the polymerization follows the controlled progression of NMP. The NER experiments and respective analysis via EPR spectroscopy confirm that the TEMPO groups remain on the surface and retain their reactivity throughout the modifications. The surface modification with polystyrene significantly improves the surface properties of UiO 66 NH_2 NPs while retaining their crystalline structures. Increasing the degree of polymerization increases the stability of suspensions in apolar solvents up to a point where it is difficult to collect the particles via centrifugation while being suspended in toluene. We anticipate that the activity of the alkoxyamine functions on the surface, which prevails even after polymerization, will serve as a versatile tool to create advanced macromolecular structures such as block copolymers and to dynamically modify the surface properties of MOFs on demand, using smart alkoxyamines. The alkoxyamine used in our approach limits monomers to styrene and some derivates thereof. However, the limitation is mainly due to the nitroxide moiety. Changing to other nitroxide moieties offers a broad spectrum of modifications. Our surface modification method, therefore, provides a versatile tool to integrate MOFs in advanced applications such as smart drug delivery systems or imaging agents or as fillers in membrane applications.[45]

AUTHOR INFORMATION

Corresponding Author

Manuel Tsotsalas − *Institute of Functional Interfaces (IFG), Karlsruhe Institute of Technology (KIT), 76344 Eggenstein Leopoldshafen, Germany; Institute of Organic Chemistry (IOC), Karlsruhe Institute of Technology (KIT), 76131 Karlsruhe, Germany;* orcid.org/0000 0002 9557 2903; Email: manuel.tsotsalas@kit.edu

Authors

Simon Spiegel − *Institute of Functional Interfaces (IFG), Karlsruhe Institute of Technology (KIT), 76344 Eggenstein Leopoldshafen, Germany*

Ilona Wagner − *Institute of Functional Interfaces (IFG), Karlsruhe Institute of Technology (KIT), 76344 Eggenstein Leopoldshafen, Germany*

Salma Begum − *Institute of Functional Interfaces (IFG), Karlsruhe Institute of Technology (KIT), 76344 Eggenstein Leopoldshafen, Germany; 3DMM2O—Cluster of Excellence (EXC 2082/1 390761711), Karlsruhe Institute of Technology (KIT), 76131 Karlsruhe, Germany; Institute of Organic Chemistry (IOC), Karlsruhe Institute of Technology (KIT), 76131 Karlsruhe, Germany;* orcid.org/0000 0001 9919 3073

Matthias Schwotzer − *Institute of Functional Interfaces (IFG), Karlsruhe Institute of Technology (KIT), 76344 Eggenstein Leopoldshafen, Germany*

Isabelle Wessely − *3DMM2O—Cluster of Excellence (EXC 2082/1 390761711), Karlsruhe Institute of Technology (KIT), 76131 Karlsruhe, Germany; Institute of Organic Chemistry (IOC), Karlsruhe Institute of Technology (KIT), 76131 Karlsruhe, Germany*

Stefan Bräse − *3DMM2O—Cluster of Excellence (EXC 2082/1 390761711), Karlsruhe Institute of Technology (KIT), 76131 Karlsruhe, Germany; Institute of Organic Chemistry (IOC), Karlsruhe Institute of Technology (KIT), 76131 Karlsruhe, Germany; Institute of Biological and Chemical Systems (IBCS FMS), Karlsruhe Institute of Technology (KIT), 76344 Eggenstein Leopoldshafen, Germany*

Author Contributions

All authors have given approval to the final version of the manuscript.

Funding

German Research Foundation (DFG): Cooperative Research Centre "Molecular Structuring of Soft Matter" (SFB 1176) and Cluster "3D Matter Made to Order" (3DMM2O—EXC 2082—390761711); Helmholtz Association: Initiative and Networking Fund (VH NG 1147).

Notes

The authors declare no competing financial interest.

ACKNOWLEDGMENTS

This research work was supported by the Helmholtz Association Program at the Karlsruhe Institute of Technology. The Deutsche Forschungsgemeinschaft (DFG, German Research Foundation) in the framework of Cooperative Research Centre "Molecular Structuring of Soft Matter" (Sonderforschungbereich SFB 1176) and the Cluster "3D Matter Made to Order" under Germany's Excellence Strategy (3DMM2O—EXC 2082—390761711, Thrust A1 and A2) is greatly acknowledged for financial contributions. M.T. grate fully acknowledges the Helmholtz Association's Initiative and Networking Fund (grant VH NG 1147) for financial contributions. The authors thank Birgit Huber (Soft Matter Synthesis Laboratories at IBG3, KIT) for providing support in SEC measurements. They also thank Dr. Alexander Welle (IFG, KIT) for performing ToF SIMS measurements and Dr. Peter Weidler for support in argon sorption measurements.

REFERENCES

(1) Férey, G. Hybrid porous solids: past, present, future. *Chem. Soc. Rev.* **2008**, *37*, 191−214.

(2) Furukawa, H.; Cordova, K. E.; O'Keeffe, M.; Yaghi, O. M. The chemistry and applications of metal organic frameworks. *Science* **2013**, *341*, No. 1230444.

(3) Dhakshinamoorthy, A.; Opanasenko, M.; Cejka, J.; Garcia, H. Metal Organic Frameworks as Solid Catalysts in Condensation Reactions of Carbonyl Groups. *Adv. Synth. Catal.* **2013**, *355*, 247−268.

(4) Zhang, W.; Huang, R.; Song, L.; Shi, X. Cobalt based metal organic frameworks for the photocatalytic reduction of carbon dioxide. *Nanoscale* **2021**, *13*, 9075−9090.

(5) So, M. C.; Wiederrecht, G. P.; Mondloch, J. E.; Hupp, J. T.; Farha, O. K. Metal organic framework materials for light harvesting and energy transfer. *Chem. Commun.* **2015**, *51*, 3501−3510.

(6) Dong, R.; Han, P.; Arora, H.; Ballabio, M.; Karakus, M.; Zhang, Z.; Shekhar, C.; Adler, P.; Petkov, P. S.; Erbe, A.; Mannsfeld, S. C. B.; Felser, C.; Heine, T.; Bonn, M.; Feng, X.; Canovas, E. High mobility band like charge transport in a semiconducting two dimensional metal organic framework. *Nat. Mater.* **2018**, *17*, 1027−1032.

(7) Stassen, I.; Burtch, N.; Talin, A.; Falcaro, P.; Allendorf, M.; Ameloot, R. An updated roadmap for the integration of metal organic frameworks with electronic devices and chemical sensors. *Chem. Soc. Rev.* **2017**, *46*, 3185−3241.

(8) Li, H.; Wang, K. C.; Sun, Y. J.; Lollar, C. T.; Li, J. L.; Zhou, H. C. Recent advances in gas storage and separation using metal organic frameworks. *Mater. Today* **2018**, *21*, 108−121.

(9) Simon Yarza, T.; Mielcarek, A.; Couvreur, P.; Serre, C. Nanoparticles of Metal Organic Frameworks: On the Road to In Vivo Efficacy in Biomedicine. *Adv. Mater.* **2018**, *30*, No. 1707365.

(10) Ploetz, E.; Engelke, H.; Lächelt, U.; Wuttke, S. The Chemistry of Reticular Framework Nanoparticles: MOF, ZIF, and COF Materials. *Adv. Funct. Mater.* **2020**, *30*, No. 1909062.

(11) Cai, W.; Wang, J.; Chu, C.; Chen, W.; Wu, C.; Liu, G. Metal Organic Framework Based Stimuli Responsive Systems for Drug Delivery. *Adv. Sci.* **2019**, *6*, No. 1801526.

(12) Nasrabadi, M.; Ghasemzadeh, M. A.; Monfared, M. R. Z. The preparation and characterization of UiO 66 metal organic frameworks for the delivery of the drug ciprofloxacin and an evaluation of their antibacterial activities. *New J. Chem.* **2019**, *43*, 16033−16040.

(13) Forgan, R. S. The surface chemistry of metal organic frameworks and their applications. *Dalton Trans.* **2019**, *48*, 9037−9042.

(14) Chen, X.; Zhuang, Y.; Rampal, N.; Hewitt, R.; Divitini, G.; O'Keefe, C. A.; Liu, X.; Whitaker, D. J.; Wills, J. W.; Jugdaohsingh, R.; Powell, J. J.; Yu, H.; Grey, C. P.; Scherman, O. A.; Fairen Jimenez, D. Formulation of Metal−Organic Framework Based Drug Carriers by Controlled Coordination of Methoxy PEG Phosphate: Boosting Colloidal Stability and Redispersibility. *J. Am. Chem. Soc.* **2021**, *143*, 13557−13572.

(15) Tanh Jeazet, H. B.; Staudt, C.; Janiak, C. Metal organic frameworks in mixed matrix membranes for gas separation. *Dalton Trans.* **2012**, *41*, 14003−14027.

(16) Kalaj, M.; Bentz, K. C.; Ayala, S.; Palomba, J. M.; Barcus, K. S.; Katayama, Y.; Cohen, S. M. MOF Polymer Hybrid Materials: From

Simple Composites to Tailored Architectures. *Chem. Rev.* **2020**, *120*, 8267−8302.
(17) Kitao, T.; Zhang, Y.; Kitagawa, S.; Wang, B.; Uemura, T. Hybridization of MOFs and polymers. *Chem. Soc. Rev.* **2017**, *46*, 3108−3133.
(18) Lin, R.; Ge, L.; Hou, L.; Strounina, E.; Rudolph, V.; Zhu, Z. Mixed matrix membranes with strengthened MOFs/polymer interfacial interaction and improved membrane performance. *ACS Appl. Mater. Interfaces* **2014**, *6*, 5609−5618.
(19) Shen, J.; Liu, G. P.; Huang, K.; Li, Q. Q.; Guan, K. C.; Li, Y. K.; Jin, W. Q. UiO 66 polyether block amide mixed matrix membranes for CO2 separation. *J. Membr. Sci.* **2016**, *513*, 155−165.
(20) Wang, S.; McGuirk, C. M.; d'Aquino, A.; Mason, J. A.; Mirkin, C. A. Metal−Organic Framework Nanoparticles. *Adv. Mater.* **2018**, *30*, No. 1800202.
(21) Wang, Z.; Cohen, S. M. Postsynthetic modification of metal organic frameworks. *Chem. Soc. Rev.* **2009**, *38*, 1315−1329.
(22) Nayab, S.; Trouillet, V.; Gliemann, H.; Weidler, P. G.; Azeem, I.; Tariq, S. R.; Goldmann, A. S.; Barner Kowollik, C.; Yameen, B. Reversible Diels Alder and Michael Addition Reactions Enable the Facile Postsynthetic Modification of Metal Organic Frameworks. *Inorg. Chem.* **2021**, *60*, 4397−4409.
(23) Audran, G.; Bremond, P.; Marque, S. R. Labile alkoxyamines: past, present, and future. *Chem. Commun.* **2014**, *50*, 7921−7928.
(24) Tebben, L.; Studer, A. Nitroxides: applications in synthesis and in polymer chemistry. *Angew. Chem., Int. Ed.* **2011**, *50*, 5034−5068.
(25) Nicolas, J.; Guillaneuf, Y.; Lefay, C.; Bertin, D.; Gigmes, D.; Charleux, B. Nitroxide mediated polymerization. *Prog. Polym. Sci.* **2013**, *38*, 63−235.
(26) Shipp, D. A. Reversible Deactivation Radical Polymerizations. *Polym. Rev.* **2011**, *51*, 99−103.
(27) Grubbs, R. B. Nitroxide Mediated Radical Polymerization: Limitations and Versatility. *Polym. Rev.* **2011**, *51*, 104−137.
(28) Wagner, H.; Brinks, M. K.; Hirtz, M.; Schafer, A.; Chi, L.; Studer, A. Chemical surface modification of self assembled mono layers by radical nitroxide exchange reactions. *Chem. Eur. J.* **2011**, *17*, 9107−9112.
(29) Lamontagne, H. R.; Lessard, B. H. Nitroxide Mediated Polymerization: A Versatile Tool for the Engineering of Next Generation. *ACS Appl. Polym. Mater.* **2020**, *2*, 5327−5344.
(30) Rowan, S. J.; Cantrill, S. J.; Cousins, G. R.; Sanders, J. K.; Stoddart, J. F. Dynamic covalent chemistry. *Angew. Chem., Int. Ed.* **2002**, *41*, 898−952.
(31) Wessely, I.; Mugnaini, V.; Bihlmeier, A.; Jeschke, G.; Brase, S.; Tsotsalas, M. Radical exchange reaction of multi spin isoindoline nitroxides followed by EPR spectroscopy. *RSC Adv.* **2016**, *6*, 55715−55719.
(32) Schulte, B.; Tsotsalas, M.; Becker, M.; Studer, A.; De Cola, L. Dynamic microcrystal assembly by nitroxide exchange reactions. *Angew. Chem., Int. Ed.* **2010**, *49*, 6881−6884.
(33) Otsuka, H. Reorganization of polymer structures based on dynamic covalent chemistry: polymer reactions by dynamic covalent exchanges of alkoxyamine units. *Polym. J.* **2013**, *45*, 879−891.
(34) An, Q.; Wessely, I. D.; Matt, Y.; Hassan, Z.; Brase, S.; Tsotsalas, M. Recycling and self healing of dynamic covalent polymer networks with a precisely tuneable crosslinking degree. *Polym. Chem.* **2019**, *10*, 672−678.
(35) Wessely, I. D.; Matt, Y.; An, Q.; Brase, S.; Tsotsalas, M. Dynamic porous organic polymers with tuneable crosslinking degree and porosity. *RSC Adv.* **2021**, *11*, 27714−27719.
(36) Jia, Y.; Matt, Y.; An, Q.; Wessely, I.; Mutlu, H.; Theato, P.; Bräse, S.; Llevot, A.; Tsotsalas, M. Dynamic covalent polymer networks via combined nitroxide exchange reaction and nitroxide mediated polymerization. *Polym. Chem.* **2020**, *11*, 2502−2510.
(37) Cavka, J. H.; Jakobsen, S.; Olsbye, U.; Guillou, N.; Lamberti, C.; Bordiga, S.; Lillerud, K. P. A new zirconium inorganic building brick forming metal organic frameworks with exceptional stability. *J. Am. Chem. Soc.* **2008**, *130*, 13850−13851.
(38) Kandiah, M.; Nilsen, M. H.; Usseglio, S.; Jakobsen, S.; Olsbye, U.; Tilset, M.; Larabi, C.; Quadrelli, E. A.; Bonino, F.; Lillerud, K. P. Synthesis and Stability of Tagged UiO 66 Zr MOFs. *Chem. Mater.* **2010**, *22*, 6632−6640.
(39) Cohen, S. M. Postsynthetic methods for the functionalization of metal organic frameworks. *Chem. Rev.* **2012**, *112*, 970−1000.
(40) Costa, J. S.; Gamez, P.; Black, C. A.; Roubeau, O.; Teat, S. J.; Reedijk, J. Chemical modification of a bridging ligand inside a metal organic framework while maintaining the 3D structure. *Eur. J. Inorg. Chem.* **2008**, *2008*, 1551−1554.
(41) Le, D.; Phan, T. N. T.; Autissier, L.; Charles, L.; Gigmes, D. A well defined block copolymer synthesis via living cationic polymer ization and nitroxide mediated polymerization using carboxylic acid based alkoxyamines as a dual initiator. *Polym. Chem.* **2016**, *7*, 1659−1667.
(42) Schaate, A.; Roy, P.; Godt, A.; Lippke, J.; Waltz, F.; Wiebcke, M.; Behrens, P. Modulated synthesis of Zr based metal organic frameworks: from nano to single crystals. *Chem. Eur. J.* **2011**, *17*, 6643−6651.
(43) Kandiah, M.; Usseglio, S.; Svelle, S.; Olsbye, U.; Lillerud, K. P.; Tilset, M. Post synthetic modification of the metal organic framework compound UiO 66. *J. Mater. Chem.* **2010**, *20*, 9848−9851.
(44) Katz, M. J.; Brown, Z. J.; Colón, Y. J.; Siu, P. W.; Scheidt, K. A.; Snurr, R. Q.; Hupp, J. T.; Farha, O. K. A facile synthesis of UiO 66, UiO 67 and their derivatives. *Chem. Commun.* **2013**, *49*, 9449−9451.
(45) Audran, G.; Marque, S. R. A.; Mellet, P. Smart Alkoxyamines: A New Tool for Smart Applications. *Acc. Chem. Res.* **2020**, *53*, 2828−2840.